Radiation resistant metal–organic frameworks for the production of high specific activity 51Cr by the Szilard-Chalmers effect

Ma, Chao; Sánchez-García, Iván; Wang, Runze; Galán, Hitos; Denkova, Antonia G.; Serra Crespo, Pablo

DOI
10.1016/j.seppur.2024.128212

Publication date
2025

Document Version
Final published version

Published in
Separation and Purification Technology

Citation (APA)
Ma, C., Sánchez-García, I., Wang, R., Galán, H., Denkova, A. G., & Serra Crespo, P. (2025). Radiation resistant metal–organic frameworks for the production of high specific activity 51Cr by the Szilard-Chalmers effect. *Separation and Purification Technology*, *352*, Article 128212. https://doi.org/10.1016/j.seppur.2024.128212

Separation and Purification Technology 352 (2025) 128212

Contents lists available at ScienceDirect

Separation and Purification Technology

journal homepage: www.elsevier.com/locate/seppur

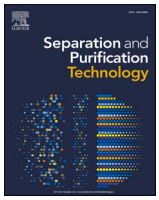

Radiation resistant metal–organic frameworks for the production of high specific activity ^{51}Cr by the Szilard-Chalmers effect

Chao Ma [a,b], Iván Sánchez-García [c], Runze Wang [b], Hitos Galán [c], Antonia G. Denkova [b], Pablo Serra Crespo [d,*]

[a] Zhongyuan Critical Metals Laboratory, Zhengzhou University, Science Road 100, Zhengzhou, Henan 450001, China
[b] Applied radiation and isotopes, Radiation Science and Technology, Faculty of applied sciences, Delft University of Technology, 2629 JB Delft, Mekelweg 15, the Netherlands
[c] Centro de Investigaciones Energéticas, Medioambientales y Tecnológicas, (CIEMAT), Avda. Complutense 40, 28040 Madrid, Spain
[d] European Commission Joint Research Centre Petten, Westerduinweg 3, NL-1755 LE Petten, the Netherlands

ARTICLE INFO

Keywords:
Metal-Organic Frameworks
Radiation Stability
Gamma Rays
^{51}Cr
Szilard-Chalmers Effect

ABSTRACT

Chromium-51 (^{51}Cr) is an attractive radionuclide for diagnosis, which is usually applied for red cells and platelet radiolabeling. However, commercially available ^{51}Cr produced in nuclear reactors via neutron activation requires long irradiation times and complex separation methods. In this work, five metal–organic frameworks (MIL-100 (Cr), MIL-100 (Fe), MIL-100 (Al), MIL-101 (Cr) and aluminium fumarate MOF (FuAl)) were synthesized and the effect of gamma ray irradiation with a high dose rate and a maximum dose of 6 MGy was investigated. The two chromium-based MOFs, MIL-100 (Cr) and MIL-101 (Cr), were selected as radiation targets to produce high specific activity ^{51}Cr by the Szilard-Chalmers effect. A solid–liquid extraction was applied to extract the produced ^{51}Cr under different conditions, including different extractants, extraction times and pH. The most promising results were achieved when using irradiated MIL-101 (Cr) and EDTA as extracting agent, reaching an enrichment factor of 1132 ± 50.

1. Introduction

Chromium-51 (^{51}Cr) is an attractive radionuclide for special diagnostic procedures in nuclear medicine due to its half-life (27.7 days) and decay by electron capture, with the emission of gamma photons with an energy of 320.1 keV. ^{51}Cr is commonly used to radiolabel red blood cells and platelets allowing to assess their life span or to determine the blood volume of patients as well as to diagnose gastrointestinal bleeding [1,2]. Currently, ^{51}Cr is produced by neutron activation in nuclear reactors based on the ^{50}Cr(n, γ)^{51}Cr reaction. The specific activity of ^{51}Cr needed for clinical application must be at least 1.85 TBq/g [3]. In order to produce ^{51}Cr with such high specific activity, enriched ^{50}Cr targets, high neutron flux and long irradiation times are essential [4]. However, these conditions restrict the production of high-specific activity ^{51}Cr to a few research reactors. An alternative method to produce ^{51}Cr with high specific activity is applying the Szilard-Chalmers effect. The Szilard Chalmers effect is based on the principle that upon the emission of high energy prompt gammas when neutron activated, the resulting atom can receive sufficiently high energy to break the chemical bonds in the target material so that it can be released from its initial chemical structure [5]. Provided that the produced radionuclide can be separated from the original chemical compound, radionuclides with high specific activity can be produced via this method.

In the past few decades, ^{51}Cr produced via the Szilard-Chalmers method was mainly obtained based on the irradiation of K_2CrO_4 targets [6]. For example, Brune. et al. [7] studied how ^{51}Cr could be separated using alumina carrier based on a coprecipitation method at different temperatures, showing that a ~ 72 % elution efficiency with an enrichment factor of 183 could be achieved. Vimalnath et al. [8] also utilized the same precipitation method to separate the produced ^{51}Cr, obtaining high specific activity of ^{51}Cr (5.5 TBq/g). However, the precipitation separation process requires extra experimental steps, which are time-consuming (3–5 days) and can lead to the introduction of impurities. Therefore, new targets should be explored to facilitate a very simple separation method without compromising the quality of the obtained product.

Metal-organic frameworks (MOFs) have attracted great attention due to their diverse applications, such as in catalysis [9,10], drug delivery

* Corresponding author.
E-mail address: Pablo.SERRA-CRESPO@ec.europa.eu (P. Serra Crespo).

https://doi.org/10.1016/j.seppur.2024.128212
Received 10 April 2024; Received in revised form 23 May 2024; Accepted 29 May 2024
Available online 31 May 2024

[11,12], luminescence sensing [13–15], adsorption and separation of radionuclides and capture of radioactive gas [16–22]. However, many MOFs are unattractive in the application where harsh radiation environment can be present due to their poor thermal and chemical stability [23,24]. In addition, considering the radiation environment present in a nuclear reactor, the irradiated targets should possess excellent radiation resistance. Some researchers reported the gamma radiation stability of several MOFs when exposed to gamma rays and determined the most important characteristics of these materials for ensuring good radiation stability, including crystallinity, density, surface area, aromaticity and linker connectivity [17,25–29]. Currently, the maximum dose applied was 6 MGy in order to investigate the radiation stability of a Np(V) Neptune MOF by Gilson et al [30]. The authors found that the structure of the Np(V) MOF was significantly disrupted. In previous research [31] performed by us, the gamma radiation stability of four MOFs subjected to a dose of 5 MGy was investigated at a dose rate of 0.65 kGy/h. However, much higher dose rates as well as higher doses might be relevant and should be studied for many applications. So far there is hardly any literature examining the influence of gamma dose rate on the stability of MOFs especially for high dose exposures.

Therefore, we synthesized two chromium-based Metal-Organic Frameworks (MOFs), specifically MIL-100 (Cr) and MIL-101 (Cr), alongside three additional MOFs: MIL-100 (Al), MIL-100 (Fe)—both of which possess the same crystal structure as MIL-100(Cr)—and aluminium fumarate MOF (FuAl), which lacks an aromatic linker. Our objective was to investigate their stability under high gamma radiation exposure. By selecting these 5 different MOFs, we aimed to investigate into the mechanisms of radiation-induced damage and assess the resistance of these MOFs in extreme radiation environments, such as those found in nuclear reactors (Fig. 1 (a)). In addition, MIL-100 (Cr) and MIL-101 (Cr), which have high surface area, large pores, excellent thermal, chemical and radiation stability [32,33], were investigated as irradiation target materials to produce high specific activity ^{51}Cr utilizing the Szilard Chalmers effect (Fig. 1 (b)). Different factors were investigated including extraction time, different extractants and pH values to identify the optimal ^{51}Cr extraction conditions.

2. Results and discussion

2.1. Radiation stability of MOFs

The five MOFs that were irradiated by the gamma source were characterized by XRD, TGA, FT-IR and N_2 adsorption. Fig. 2 (a) shows the XRD pattern of MIL-100 (Cr) after being exposed to different gamma doses, ranging from 0 MGy to 6 MGy. No obvious difference can be observed in the diffraction patterns and the full width at half maxima (FWHM) of MIL-100 (Cr) did not have a significant change except for a small variation of around 3 % (Fig. 2 (f)), indicating that MIL-100 (Cr) still retained good crystallinity after having received 6 MGy of gamma radiation. The XRD pattern of MIL-101 (Cr) irradiated up to 5 MGy displayed no changes compared to the unirradiated MIL-101 (Cr) (Fig. 2 (b)). However, after 5 MGy of gamma radiation, the diffraction peaks of MIL-101 (Cr) became broader and less intense. The FWHM had a significant increase of 27 % after receiving 6 MGy radiation, indicating a decrease in crystallinity. To further reveal the effect of metal clusters on the radiation stability of MOFs, MIL-100 (Fe) and MIL-100 (Al), which have the same crystal structure and organic linker but different metals compared to MIL-100 (Cr), were also characterized by XRD after exposure to different gamma doses. MIL-100 (Fe) exhibited almost no variation in the diffraction patterns (Fig. 2 (c)) and its FWHM only had 2.8 % decrease from 0 to 6 MGy, showing no considerable crystal degradation. For MIL-100 (Al), its crystallinity started degrading after receiving 4 MGy of gamma radiation (Fig. 2 (d)) with 9.6 % increase in its FWHM. Additionally, the XRD pattern of FuAl MOF, which has the same metal clusters but different organic linkers compared to MIL-100 (Al), was recorded, as shown in Fig. 2 (e). Their FWHM showed gradual increase (3 %) with increasing gamma dose up to 2 MGy, i.e. the maximum dose that the material managed to resist before becoming amorphous.

To further monitor the structural changes of the MOFs after gamma radiation, their BET surface area and pore volumes were determined by N_2 adsorption. Fig. 3 (a) shows the N_2 adsorption isotherms of MIL-100 (Cr) at different accumulated gamma doses. The BET surface area of the irradiated MIL-100 (Cr) decreased from 1862 m^2/g to 1487 m^2/g, showing 20.1 % descent in surface area after an accumulated dose of 6 MGy, which is consistent with the reduction of its micropore volume (21.7 %, Fig. 3 (f)). MIL-101 (Cr) decreased by 24.4 % in surface area (1665 m^2/g) after receiving a gamma dose of 6 MGy (Fig. 3 (b)). Its micropore volume decreased from 1.0715 cm^3/g to 0.6707 cm^3/g (a 37.4 % reduction). This significant reduction indicated that the partial pore structure of the MOFs had collapsed. Meanwhile, MIL-100 (Fe) and MIL-100 (Al) possessed better gamma radiation stability, i.e. their BET surface area only decreased by 3.9 % and 12.9 % and the micropore volume decreased by 17 % and 6.6 %, respectively. Furthermore, the FuAl MOF had a decrease of 52.9 % in surface area and decrease of 46.1 % in micropore volume after gamma radiation of 2 MGy, displaying poorer resistance towards gamma irradiation.

To explore the effects of gamma radiation on the MOFs, infrared spectroscopy was employed to obtain more insights into their structural

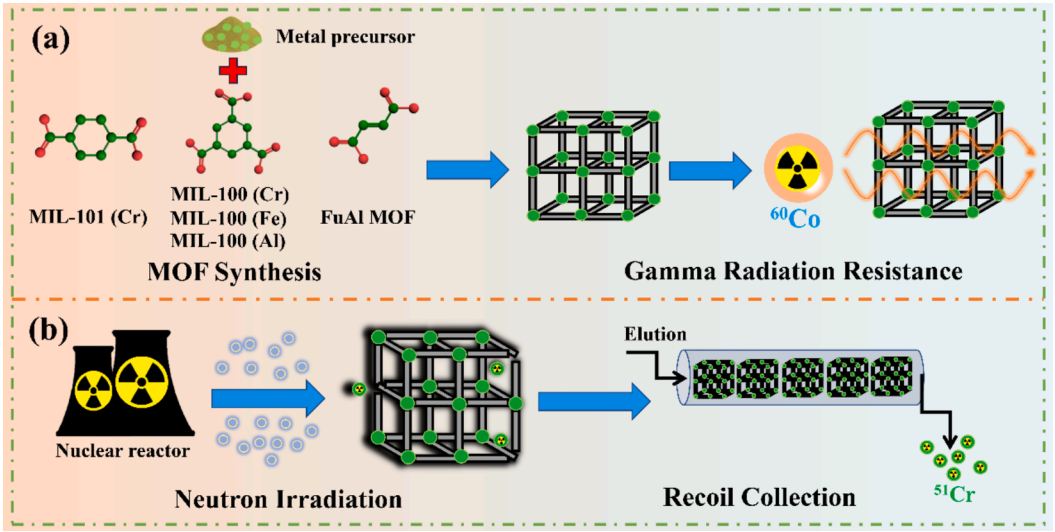

Fig. 1. Schematic diagram of (a) gamma radiation stability of five MOFs and (b) high specific activity ^{51}Cr production.

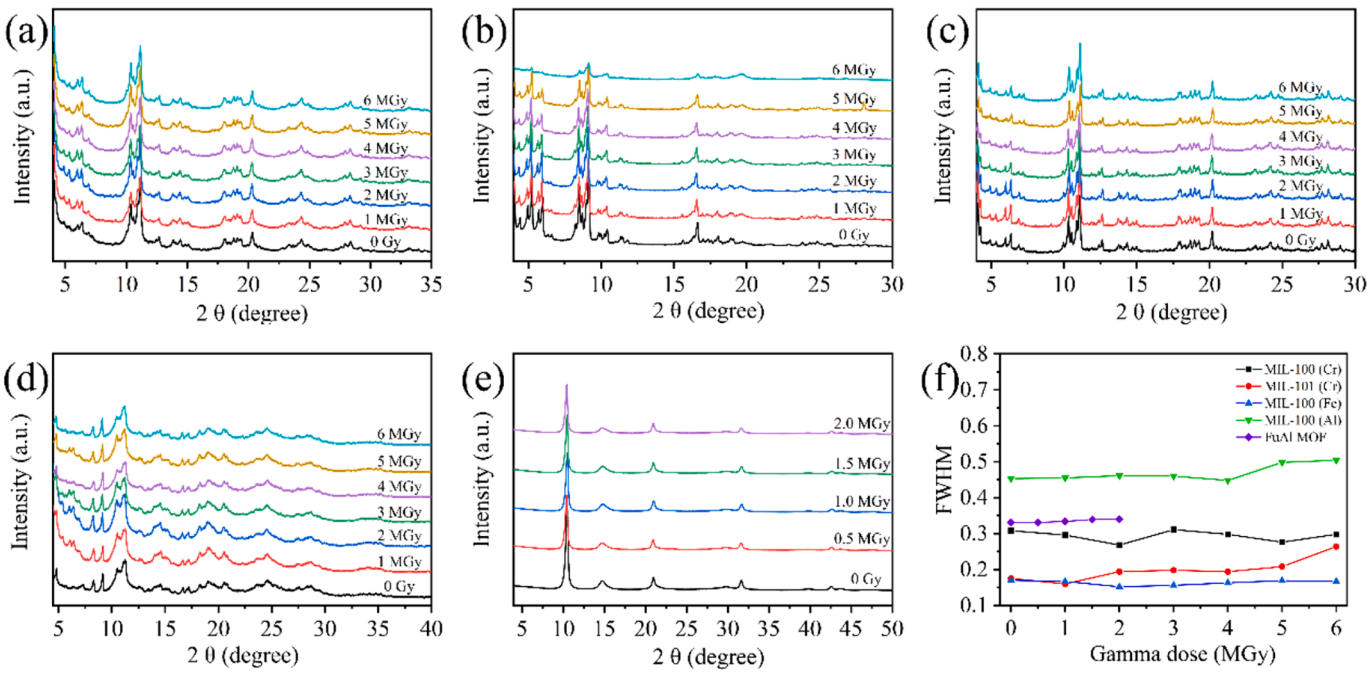

Fig. 2. XRD patterns of (a) MIL-100 (Cr), (b) MIL-101 (Cr), (c) MIL-100 (Fe), (d) MIL-100 (Al) and (e) FuAl MOF; (f) the FWHM of all MOFs after exposure to different doses of gamma radiation.

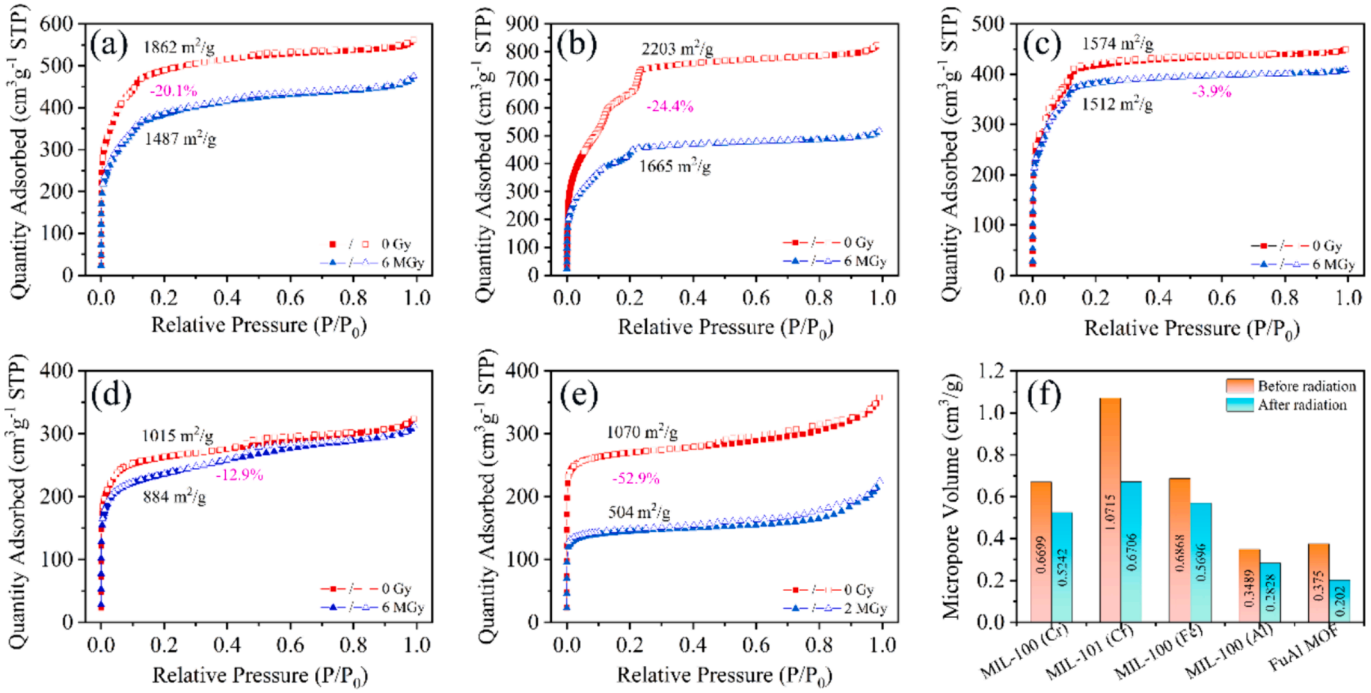

Fig. 3. N_2 adsorption isotherms of (a) MIL-100 (Cr), (b) MIL-101 (Cr), (c) MIL-100 (Fe), (d) MIL-100 (Al) and (e) FuAl MOF before and after gamma radiation; (f) Comparison of micropore volume of all MOFs before and after gamma radiation.

decomposition. The IR spectra of three MIL-100 MOFs after irradiation are similar to the pristine MOFs and no noticeable band shifts and in-growths can be observed (Figs. S2–S4). However, the intensity of the peak for MIL-101 (Cr) at around 720 cm^{-1} attributed to Cr-O bonds [34] attenuated gradually and disappeared completely at 6 MGy irradiation (Fig. S5), indicating that some connection nodes between chromium clusters and organic linkers were broken, which is consistent with the XRD results. For the FuAl MOF, the peak at around 710 cm^{-1} assigned to the stretching vibration of O-Al groups [35] could not be observed after 2 MGy gamma irradiation (Fig. S6), displaying a similar behaviour as MIL-101 (Cr).

Moreover, thermogravimetric analysis was applied to evaluate the decomposition temperature of MOFs after gamma irradiation. After receiving gamma irradiation of 6 MGy, the structural decomposition of MIL-100 (Cr) and MIL-101 (Cr) shifted lower temperatures (Figs. S7 and S8), indicating that their decomposition temperature decreased after 6 MGy irradiation. More shifts could be observed in the TG curve of MIL-101 (Cr), showing worse robustness, which is consistent with the BET

results. TG curves of MIL-100 (Fe) and MIL-100 (Al) are displayed in Fig. S9 and Fig. S10, respectively. No major changes could be found suggesting that the temperature resistance was not altered after 6 MGy of gamma irradiation. Furthermore, the decomposition temperature of the FuAl MOF decreased gradually (Fig. S10), displaying severe structural damage.

Based on the above experimental results, the trend of gamma radiation stability can be summarized as MIL-100 (Fe) > MIL-100 (Al) > MIL-100 (Cr) > MIL-101 (Cr) > FuAl MOF. The interaction of gamma rays with matter is primarily governed by three processes: the photoelectric effect, the Compton effect, and pair production. The likelihood of these interactions occurring is highly influenced by the gamma ray's energy and the atomic number (Z) of the matter. Among these, the Compton effect is anticipated to be the predominant mechanism for gamma rays with energies of 1.17 and 1.33 MeV, especially in materials made of elements with the specific Z values found in Metal-Organic Frameworks (MOFs). This process involves gamma rays transferring part of their energy to an electron within the MOF, leading to the gamma ray losing energy. This energy reduction allows the gamma ray to potentially engage in further interactions, such as subsequent Compton effects or the photoelectric effect, thereby producing recoil electrons (illustrated in Fig. 5 (a)). Some of these Compton-generated electrons might escape into the air without interacting further, while others may collide with electrons in atoms within the MOFs. These collisions, characterized by incoherent scattering, can result in ionization or excitation of atoms. The excited atoms can then release their energy through the emission of fluorescence or Auger electrons and, ultimately, convert it into vibrational energy (heat dissipation) [36,37].

The FuAl MOF exhibited the worst gamma radiation stability, which could be attributed to the presence of non-aromatic organic ligands. Aromatic linkers facilitate the spread and movement of excited states due to their capacity for high-energy delocalization. As a result, the aromatic nature of these linkers plays a crucial role in enhancing the stability of Metal-Organic Frameworks (MOFs) when exposed to gamma radiation. When compared to the three MIL-100 MOFs, MIL-101 (Cr) had a more pronounced BET surface area reduction after irradiation, exhibiting worse radiation stability, which could be related to the linker connectivity. When two connection sites of one linker in MIL-101 (Cr) are destroyed, the structure starts collapsing, affecting the crystallinity and porosity of the material. On the other hand, MIL-100 had three linker connection sites and the whole structure could still be maintained when two connection sites are broken. In addition, the three MIL-100 MOFs have the same organic linkers and crystal structure but contain different metals and show different radiation resistance performance. To understand their difference in radiation stability, the absorption cross-section of those metals is examined (see Fig. S12). From this figure it can be seen that the cross-section of chromium and iron are similar and higher than that of aluminum, which means that the cross-section of the metals is not the most important factor for the radiation stability of MOFs. One possible factor can be the defects in the MOFs, such as ligand and metal node defects, resulting in the loss of local linker and node connectivity. Compared to our previous study [31], similar results were acquired, although much higher dose and dose rate were applied in this study. Based on the observations it is suggested that the dose rate at which radiation is administered does not significantly impact the structural integrity of the studied MOFs until the cumulative radiation exposure surpasses a critical threshold dose, at which point decomposition of the MOF structure commences.

Therefore, to produce ^{51}Cr with high specific activity, the maximum gamma dose received by the irradiatied targets should be in accordance with their resistivity. The gamma dose rate in the HOR nuclear reactor and the BP3 irradiation facility is around 300 kGy/h. According to our research results, MIL-100 (Cr) and MIL-100 (Cr) exhibit prominent stability up to a gamma dose of 5 MGy. The maximum radiation time in the BP3 facility is 10 h resulting in a total gamma dose of 3 MGy received by the two chromium-based MOFs, which is below the limit of their radiation resistance.

2.2. ^{51}Cr extraction

2.2.1. Optimized ^{51}Cr extraction for MIL-100 (Cr)

MIL-100 (Cr) was used as target to produce ^{51}Cr with high specific activity. To find the optimized extraction conditions of ^{51}Cr for MIL-100 (Cr), the extraction based on the Szilard-Chalmers effect was performed after different contact times, EDTA concentration and pH of the solution. The effect of extraction time on the separation efficiency of ^{51}Cr is shown in Fig. 4 (a). The extraction efficiency of ^{51}Cr increased from 22 % to 33 % by increasing the extraction time from 1 h to 24 h. However, the enrichment factor (Fig. 4 (b)) decreased from 321 ± 62 to 198 ± 50 with increasing extraction time. The optimum extraction time appeared to be one hour, which resulted in an enrichment factor of 321 ± 62. The influence of EDTA concentration on the extraction efficiency was also evaluated, as shown in Fig. 4 (d). When the EDTA concentration increased from 1 mM to 100 mM, the extraction efficiency of ^{51}Cr doubled from 22 % to 46 %. Increasing further the EDTA concentration to 250 mM did not lead to improvement of the yield (45 %). The corresponding enrichment factor of ^{51}Cr was found to be the highest at 1 mM EDTA. Since the enrichment factor (EF) is considered to be the most important factor, the optimum EDTA concentration was determined to be 1 mM although the extraction efficiency was just 22 %. Furthermore, the influence of pH on the separation yield and enrichment factor was investigated, as shown in Fig. 4 (g). The extraction efficiency of ^{51}Cr decreased from 38 % to 21 % when the pH was increased from 1 to 8. The enrichment factor of ^{51}Cr was also found to be the highest at lower pH values, reaching a value of 564 ± 140. Based on the analysis mentioned above, the optimized extraction condition is using EDTA with a concentration of 1 mM at pH 1 and extraction time of 1 h.

The influence of using two different acid solutions as extractants, as well as the extraction time, was also evaluated. Fig. 5(a) shows that 82 % of ^{51}Cr could be extracted using HCl versus 57 % when applying H_2SO_4 at a fixed extraction time of 1 h. The corresponding enrichment factors were 458 ± 30 and 428 ± 195, respectively. The corresponding specific activities were 174 GBq/g and 151 GBq/g, respectively. Extending the extraction time to 24 h, the extraction efficiencies decreased to 54 % and 51 % for HCl and H_2SO_4 respectively. The EF for HCl was also found to decrease from 458 ± 30 to 207 ± 9 after 24 h of extraction. The specific activity found when using HCl decreased to 153 ± 9 GBq/g, while the specific activity when using H_2SO_4 became 271 ± 2 GBq/g. However, the specific activity when using EDTA was 126 ± 31 GBq/g and 70 ± 1 GBq/g after 1 h and 24 h extraction, respectively.

2.2.2. ^{51}Cr extraction from irradiated MIL-101 (Cr)

Fig. 6 (a) displays the extraction efficiency of MIL-101 (Cr) using three different chemical reagents at 1 h. From this figure it can be observed that 57 % of ^{51}Cr can be extracted using HCl and H_2SO_4, while a relatively higher enrichment factor of 670 ± 121 can be achieved using H_2SO_4 compared with that of HCl (552 ± 116). When EDTA was applied for ^{51}Cr extraction, a much higher enrichment factor (1132 ± 50) and specific activity (351 ± 79 GBq/g) could be obtained although it has a lower extraction efficiency (22 %). This high enrichment factor is similar to the one previously reported that has an enrichment factor of 1150 [6], however this separation method is simpler and faster..

2.2.3. ^{51}Cr production discussion

Considering the practical application of ^{51}Cr in nuclear medicine, a specific activity of ^{51}Cr (1 TBq/g) needs to be produced, however this method has been able to produce a specific activity of 351 ± 79 GBq/g, only around three times lower than desired. This was accomplished by irradiating for short time in a low-power research reactor and using non-enriched chromium. Our developed method significantly enhances the production of ^{51}Cr, addressing several critical bottlenecks. Most significantly, the separation process after irradiation is vastly simplified, and

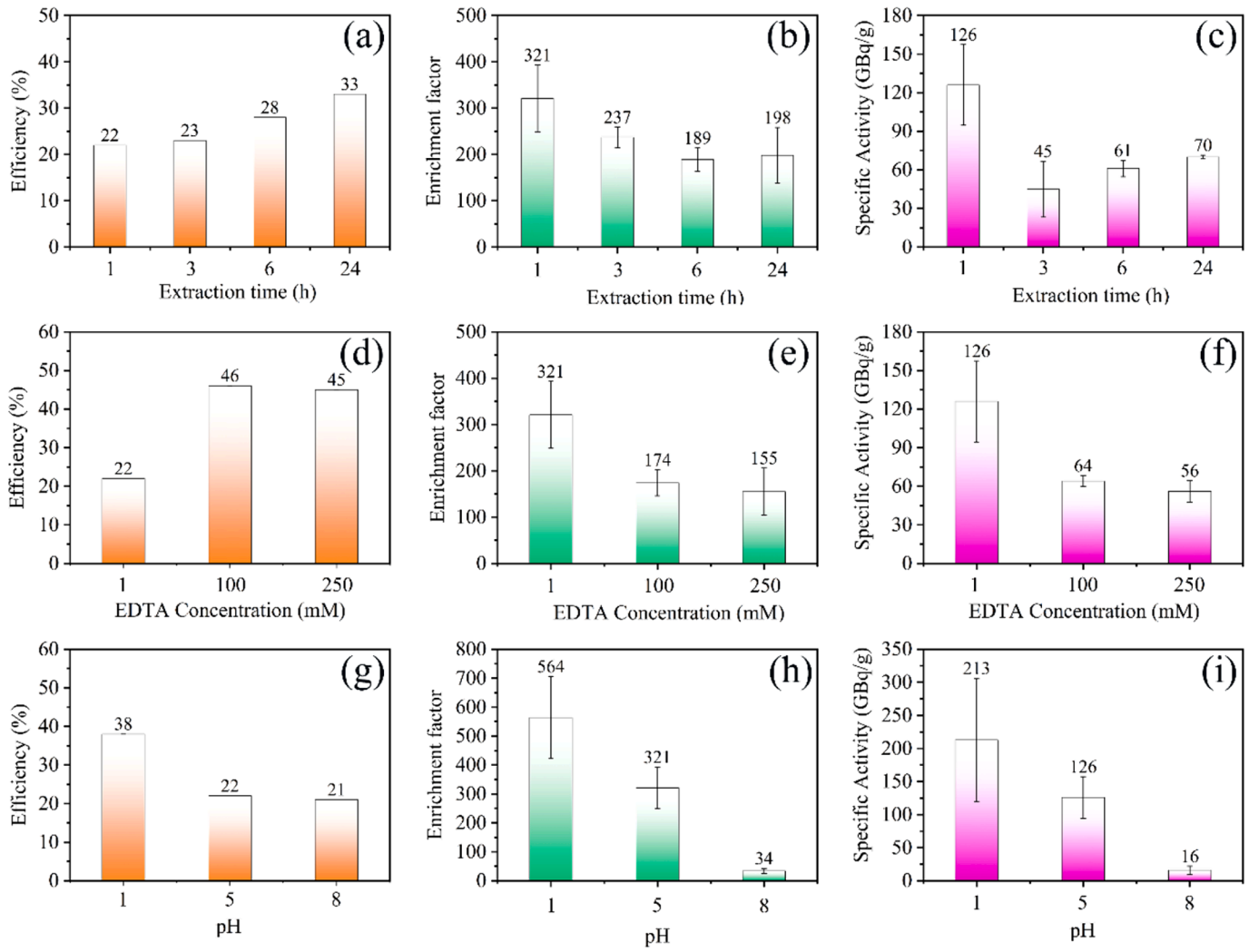

Fig. 4. Extraction efficiency (a), enrichment factor (b) and specific activity (c) of ^{51}Cr for MIL-100 (Cr) using EDTA (1 mM, pH = 5) as function of extraction time; Extraction efficiency (d), enrichment factor (e) and specific activity (f) of ^{51}Cr for MIL-100 (Cr) using EDTA (extraction time 1 h, pH = 5) as function of the EDTA concentration; Extraction efficiency (g), enrichment factor (h) and specific activity (i) of ^{51}Cr for MIL-100 (Cr) using EDTA (1 mM, extraction time 1 h) as function of the pH.

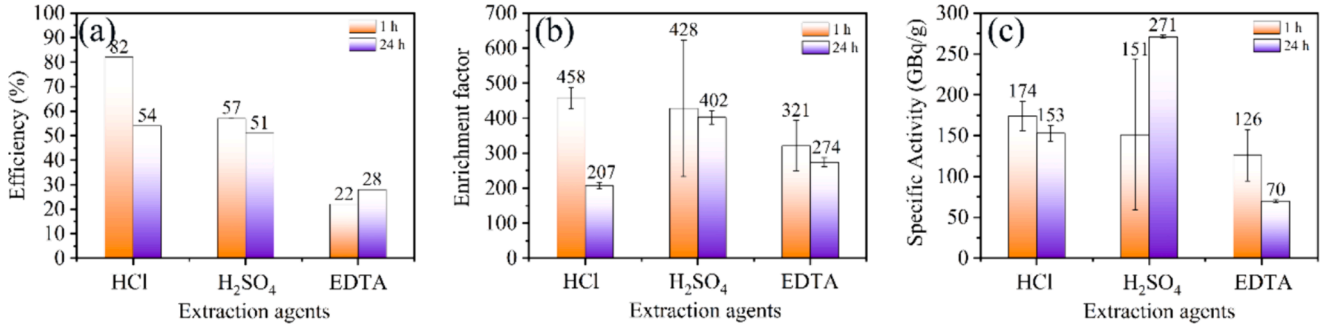

Fig. 5. (a) Efficiency, (b) enrichment factor and (c) specific activity of ^{51}Cr extracted with different extracting solutions (30 % HCl, 15 % H_2SO_4 and EDTA (1 mM, pH = 5)) at different extraction times from irradiated MIL-100 (Cr).

only takes one step, being the solid–liquid extraction, what shortens and simplifies the process compared to the reported methods based on the irradiation of K_2CrO_4. In addition, the current ^{51}Cr production methods involve, long irradiation in high flux reactors what it is not required for our method, opening the possibility for more facilities to produce ^{51}Cr. Finally, the use of enriched ^{50}Cr is not a requirement making the process more economical and easier to implement but it could be applied to easily increase the specific activity.

By optimizing irradiation conditions, employing MOFs as target material and carrying out a solid to liquid separation technique, we have successfully circumvented the challenges associated with neutron source availability, the need for enriched target materials, and the complexities

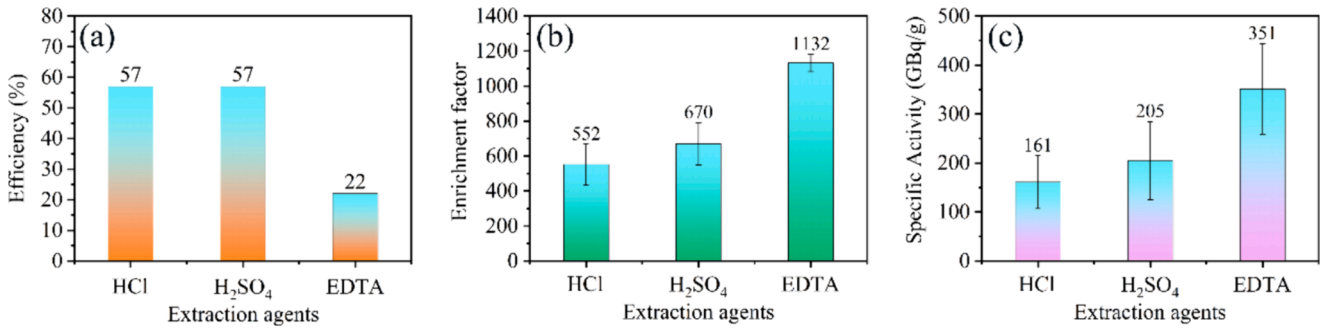

Fig. 6. (a) Efficiency, (b) enrichment factor and (c) specific activity of ^{51}Cr extracted using HCl, H_2SO_4 and EDTA for 1 h from irradiated MIL-101 (Cr).

of other separation methods. Our approach not only demonstrates a marked improvement in the yield and specific activity of ^{51}Cr but also proposes a more economically viable and environmentally friendly production pathway. This advancement holds promise for broader access and application of ^{51}Cr in nuclear medicine, potentially leading to more effective diagnostic and therapeutic procedures. For future studies, the scalability of this method and its adaptability to different reactor environments will be key areas of focus, aiming to further alleviate the production constraints and meet the increasing demand for high-quality ^{51}Cr in the medical field.

3. Conclusions

Five MOFs (MIL-100 (Cr), MIL-100 (Fe), MIL-100 (Al), MIL-101 (Cr) and FuAl) were prepared to study the effect of radiation exposure on their structural composition when applying high gamma dose rate. The results showed that MIL-100 (M) materials had a better gamma radiation stability compared to other MOFs, elucidating that the radiation resistance performance of MOFs can be enhanced by expanding aromatic linkers, improving linker connectivity and reducing defects.

MIL-100 (Cr) and MIL-101 (Cr) as irradiation targets were applied to produce ^{51}Cr using the Szilard-Chalmers method. Different conditions were explored to separate the produced ^{51}Cr using EDTA, HCl and H_2SO_4. For MIL-100 (Cr), the optimum conditions appear to be using 1 mM EDTA at pH 1 after an extraction time of 1 h. When HCl and H_2SO_4 were applied to separate ^{51}Cr, high extraction efficiency (>50 %) and enrichment factor (200 ~ 500) could be obtained. For irradiated MIL-101 (Cr), high extraction efficiency (>50 %) and enrichment factor (500 ~ 700) could be reached when HCl and H_2SO_4 were used to separate ^{51}Cr. Although ^{51}Cr separation had relatively lower separation efficiency (~22 %) using EDTA, a high enrichment factor (~1132 ± 50) and specific activity (~351 GBq/g) were achieved.

In conclusion, our innovative method substantially improves ^{51}Cr production, overcoming major obstacles such as limited neutron source availability, the need for enriched materials, and challenging waste management. Our approach offers a more cost-effective and environmentally sustainable solution, promising to facilitate wider use of ^{51}Cr in nuclear medicine. Future work will focus on scalability and adaptability to various reactor environments, aiming to meet the growing demand for this critical medical isotope efficiently.

4. Experimental

Five MOFs (MIL-100 (Cr), MIL-100 (Fe), MIL-100 (Al), MIL-101 (Cr) and FuAl MOF) were prepared and their characterization and synthesis conditions can be found in the Supporting Information (SI).

4.1. Gamma radiation

A pool-type ^{60}Co facility (Náyade, CIEMAT, Spain) was utilized to carry out the gamma irradiation experiments to evaluate the gamma radiation stability of the prepared MOFs, as shown in Fig. S1. The half-life of cobalt-60 (1.17, 1.33 MeV) is 5.272 years and the dose rate employed for the irradiation was 30.316 kGy/h. Around 0.2 g of the samples were sealed in glass vials and irradiated at different times to reach different doses. All samples were subjected to irradiation using gamma dose range of 0 ~ 6 MGy. More details about the irradiation procedure can be found in the Supporting Information (SI).

4.2. Neutron irradiation for the ^{51}Cr production

The synthesized MIL-100 (Cr) and MIL-101 (Cr) were irradiated for 10 h at the Hoger Onderwijs Reactor (HOR) of Delft University of Technology, the Netherlands. The thermal neutron flux and epithermal neutron flux of the irradiation facility used (BP3 were 3.11×10^{16}n/(s•m^2) and 7.2×10^{14}n/(s•m^2), respectively. 5 ± 0.1 mg of MOFs was sealed in Posthumus PE (polyethylene) capsules and then packaged in Posthumus PE rabbits for irradiation. All experiments were conducted in triplicate..

4.3. ^{51}Cr extraction

Typically, the selected irradiated samples were put into a glass tube containing 10 mL of extracting solution. Three solutions with different pH (1, 5 and 8) were selected for ^{51}Cr extraction using EDTA. The influence of EDTA concentration (1 mM, 100 mM and 250 mM) at pH 5 on ^{51}Cr separation was also studied. The mixture was shaken for various time intervals (1 h, 3 h, 6 h, 24 h) at room temperature and then 5 ml of the solution was transferred to a centrifuge tube and centrifuged for 10 min at 4000 rpm. Finally, 3 ml of the supernatant was taken and the counts of ^{51}Cr originating from the 321 keV were measured by gamma spectrometry (Wallac Wizard). In addition, hydrochloric acid (HCl, 30 %) and sulfuric acid (H_2SO_4, 95 ~ 97 %) from Sigma-Aldrich were diluted to HCl (30 %) and H_2SO_4 (15 %) by deionized water, respectively, which were used for ^{51}Cr extraction at 1 h and 24 h from irradiated MIL-100 (Cr) and MIL-101 (Cr)..

CRediT authorship contribution statement

Chao Ma: Writing - original draft, Writing – review & editing, Visualization, Validation, Methodology, Investigation, Formal analysis, Data curation. **Iván Sánchez-García:** Writing – review & editing, Methodology, Investigation, Formal analysis, Data curation. **Runze Wang:** Investigation. **Hitos Galán:** Writing – review & editing, Resources. **Antonia G. Denkova:** Writing – review & editing, Validation, Supervision, Resources, Project administration, Methodology, Formal analysis. **Pablo Serra Crespo:** Writing – review & editing, Visualization, Validation, Supervision, Resources, Project administration, Methodology, Investigation, Funding acquisition, Formal analysis, Data curation, Conceptualization.

Declaration of competing interest

The authors declare that they have no known competing financial interests or personal relationships that could have appeared to influence the work reported in this paper.

Data availability

No data was used for the research described in the article.

Acknowledgements

The work was financially supported by National Natural Science Foundation of China (52302073) and the project of Zhongyuan Critical Metals Laboratory.

Appendix A. Supplementary data

Supplementary data to this article can be found online at https://doi.org/10.1016/j.seppur.2024.128212.

References

[1] P.L. Mollison, N. Veall, The use of the isotope ^{51}Cr as a label for red cells, British J. Haematol. 1 (1955) 62–74.
[2] S.J. Carlson, A glance at the history of nuclear medicine, Acta Oncol. 34 (1995) 1095–1102.
[3] A. Cerwenka, T.M. Morgan, A.G. Harmsen, R.W. Dutton, Migration kinetics and final destination of type 1 and type 2 CD8 effector cells predict protection against pulmonary virus infection, J. Exp. Med. 189 (1999) 423–434.
[4] V. Shivarudrappa, K.V. Vimalnath, High purity materials as targets for radioisotope production: Needs and challenges, B, Mater. Sci. 28 (2005) 325–330.
[5] J.W.J. van Dorp, D.S. Mahes, P. Bode, H.T. Wolterbeek, A.G. Denkova, P. Serra-Crespo, Towards the production of carrier-free ^{99}Mo by neutron activation of ^{98}Mo in molybdenum hexacarbonyl Szilard-Chalmers enrichment, Appl. Radiat. Isot. 140 (2018) 138–145.
[6] N. Shibata, K.J. Yoshihara, Preparation of chromium-51 of a high specific activity by the szilard-chaimers process, B. Chem. Soc. Jpn. 32 (1959) 422–423.
[7] D. Brune, Separation of ^{51}Cr by means of the Szilard-Chalmers effect from potassium chromate Irradiated at low temperature, Sweden, Acta Chemica Scandinavia. 7 (1967) 20.
[8] K.V. Vimalnath, A. Rajeswari, S. Chakraborty, A. Dash, Large scale production of ^{51}Cr for medical application in a medium flux research reactor: A comparative investigation of Szilard-Chalmers process and direct (n, γ) route, Appl. Radiat. Isot. 91 (2014) 104–108.
[9] L. Zhu, X.Q. Liu, H.L. Jiang, L.B. Sun, Metal-organic frameworks for heterogeneous basic catalysis, Chem. Rev. 117 (2017) 8129–8176.
[10] Y.S. Wei, M. Zhang, R. Zou, Q. Xu, Metal-organic framework-based catalysts with single metal sites, Chem. Rev. 120 (2020) 12089–12174.
[11] I. Abánades Lázaro, R.S. Forgan, Application of zirconium MOFs in drug delivery and biomedicine, Coordin. Chem. Rev. 380 (2019) 230–259.
[12] M. Kotzabasaki, G.E. Froudakis, Review of computer simulations on anti-cancer drug delivery in MOFs, Inorg. Chem. Front. 5 (2018) 1255–1272.
[13] S. Wang, B. Sun, Z. Su, G. Hong, X. Li, Y. Liu, Q. Pan, J. Sun, Lanthanide-MOFs as multifunctional luminescent sensors, Inorg. Chem. Front. 9 (2022) 3259–3266.
[14] X. Liu, W. Liu, Y. Kou, X. Yang, Z. Ju, W. Liu, Multifunctional lanthanide MOF luminescent sensor built by structural designing and energy level regulation of a ligand, Inorg. Chem. Front. 9 (2022) 4065–4074.
[15] G.L. Yang, X.L. Jiang, H. Xu, B. Zhao, Applications of MOFs as luminescent sensors for environmental pollutants, Small 17 (2021) 2005327.
[16] D. Banerjee, C.M. Simon, A.M. Plonka, R.K. Motkuri, J. Liu, X. Chen, B. Smit, J. B. Parise, M. Haranczyk, P.K. Thallapally, Metal-organic framework with optimally selective xenon adsorption and separation, Nat. Commun. 7 (2016) 11831.
[17] S.K. Elsaidi, M.H. Mohamed, A.S. Helal, M. Galanek, T. Pham, S. Suepaul, B. Space, D. Hopkinson, P.K. Thallapally, J. Li, Radiation-resistant metal-organic framework enables efficient separation of krypton fission gas from spent nuclear fuel, Nat. Commun. 11 (2020) 3103.
[18] K. Jin, B. Lee, J. Park, Metal-organic frameworks as a versatile platform for radionuclide management, Coordin. Chem. Rev. 427 (2021) 213473.
[19] X. Chen, X. Liu, S. Xiao, W. Xue, X. Zhao, Q. Yang, A β-ray irradiation resistant MOF-based trap for efficient capture of Th(IV) ion, Sep. Purif. Technol. 297 (2022) 121517.
[20] C. Ma, A. Vasileiadis, H.T. Wolterbeek, A.G. Denkova, P. Serra Crespo, Adsorption of molybdenum on Zr-based MOFs for potential application in the ^{99}Mo/^{99m}Tc generator, Appl. Surf. Sci. 572 (2022) 151340.
[21] C. Ma, H.T. Wolterbeek, A.G. Denkova, P. Serra Crespo, A cerium-based metal-organic framework as adsorbent for the ^{99}Mo/^{99m}Tc generator, Sep. Purif. Technol. 295 (2022) 121218.
[22] C. Ma, H.T. Wolterbeek, A.G. Denkova, P. Serra Crespo, Porphyrinic metal-organic frameworks as molybdenum adsorbents for the ^{99}Mo/^{99m}Tc generator, Inorg. Chem. Front. 10 (2023) 2239–2249.
[23] M. Ding, X. Cai, H.L. Jiang, Improving MOF stability: approaches and applications, Chem. Sci. 10 (2019) 10209–10230.
[24] A.J. Howarth, Y. Liu, P. Li, Z. Li, T.C. Wang, J.T. Hupp, O.K. Farha, Chemical, thermal and mechanical stabilities of metal-organic frameworks, Nat. Rev. Mater. 1 (2016) 15018.
[25] C. Volkringer, C. Falaise, P. Devaux, R. Giovine, V. Stevenson, F. Pourpoint, O. Lafon, M. Osmond, C. Jeanjacques, B. Marcillaud, J.C. Sabroux, T. Loiseau, Stability of metal-organic frameworks under gamma irradiation, Chem. Commun. 52 (2016) 12502–12505.
[26] S.E. Gilson, M. Fairley, P. Julien, A.G. Oliver, S.L. Hanna, G. Arntz, O.K. Farha, J. A. LaVerne, P.C. Burns, Unprecedented radiation resistant thorium-binaphthol metal-organic framework, J. Am. Chem. Soc. 142 (2020) 13299–13304.
[27] S.L. Hanna, D.X. Rademacher, D.J. Hanson, T. Islamoglu, A.K. Olszewski, T. M. Nenoff, O.K. Farha, Structural features of zirconium-based metal-organic frameworks affecting radiolytic stability, Ind. Eng. Chem. Res. 59 (2020) 7520–7526.
[28] M. Fairley, S.E. Gilson, S.L. Hanna, A. Mishra, J.G. Knapp, K.B. Idrees, S. Chheda, H. Traustason, T. Islamoglu, P.C. Burns, L. Gagliardi, O.K. Farha, J.A. LaVerne, Linker contribution toward sstability of metal-organic frameworks under ionizing radiation, Chem. Mater. 33 (2021) 9285–9294.
[29] A.M. Hastings, M. Fairley, M.C. Wasson, D. Campisi, A. Sarkar, Z.C. Emory, K. Brunson, D.B. Fast, T. Islamoglu, M. Nyman, P.C. Burns, L. Gagliardi, O.K. Farha, A.E. Hixon, J.A. LaVerne, Role of metal selection in the radiation stability of isostructural M-UiO-66 metal-organic frameworks, Chem. Mater. 34 (2022) 8403–8417.
[30] S.E. Gilson, M. Fairley, S.L. Hanna, J.E.S. Szymanowski, P. Julien, Z. Chen, O. K. Farha, J.A. LaVerne, P.C. Burns, Unusual metal-organic framework topology and radiation resistance through neptunyl coordination chemistry, J. Am. Chem. Soc. 143 (2021) 17354–17359.
[31] C. Ma, H. Liu, H.T. Wolterbeek, A.G. Denkova, P. Serra Crespo, Effects of high gamma doses on the structural stability of metal-organic frameworks, Langmuir 38 (2022) 8928–8933.
[32] X. Li, J. Wang, X. Liu, L. Liu, D. Cha, X. Zheng, A.A. Yousef, K. Song, Y. Zhu, D. Zhang, Y. Han, Direct imaging of tunable crystal surface structures of MOF MIL-101 using high-resolution electron microscopy, J. Am. Chem. Soc. 141 (2019) 12021–12028.
[33] L. Wang, F. Zhang, C. Wang, Y. Li, J. Yang, L. Li, J. Li, Ethylenediamine-functionalized metal organic frameworks MIL-100 (Cr) for efficient CO_2/NO_2 separation, Sep. Purif. Technol. 235 (2020) 116219.
[34] L.L. Li, X.Q. Feng, R.P. Han, S.Q. Zang, G. Yang, Cr(VI) removal via anion exchange on a silver-triazolate MOF, J. Hazard. Mater. 321 (2017) 622–628.
[35] S. Abdi, M. Nasiri, Enhanced hydrophilicity and water flux of poly(ether sulfone) membranes in the presence of aluminum fumarate metal-organic framework nanoparticles: Preparation and characterization, ACS Appl. Mater. Interfaces 11 (2019) 15060–15070.
[36] C. Wang, O. Volotskova, K. Lu, M. Ahmad, C. Sun, L. Xing, W. Lin, Synergistic assembly of heavy metal clusters and luminescent organic bridging ligands in metal-organic frameworks for highly efficient X-ray scintillation, J. Am. Chem. Soc. 136 (2014) 6171–6174.
[37] S.B. Dhiman, G.S. Goff, W. Runde, J.A. LaVerne, Gamma and heavy ion radiolysis of ionic liquids: A comparative study, J. Nucl. Mater. 453 (2014) 182–187.